

# Representative, Synthetic model Ensembles Supporting decisions for Geothermal Field Development

Alexandros Daniilidis, Hamidreza M. Nick and David F. Bruhn

Stevinweg 1, Building 23 / PO-box 5048, Delft, The Netherlands

a.daniilidis@tudelft.nl

**Keywords:** reservoir engineering, direct use, uncertainty, hydraulic thermal

## ABSTRACT

Direct use, single doublet geothermal systems are subject to several uncertainties. Moreover, the interference between adjacent doublets becomes more important, as direct use geothermal systems transition towards multiple doublets by a single operator. Field development decisions are made at early stages, where uncertainties remain high and system behavior is not fully understood. Full field models remain large and computationally expensive for evaluating development scenarios. To address this, the use of synthetic, representative models can be applied to educate decisions at the field scale. In this analysis, a base Thermal Hydraulic reservoir model using a Finite Element Method is utilized. The model is a synthetic representation of a real geological setting for a conductive geothermal field. An ensemble of model realizations is simulated. The analysis is focused on the system lifetime by means of the cold front breakthrough and produced cumulative energy. Using multiple parameters values for reservoir properties and operational inputs we explore the system sensitivity and dynamics. This uncertainty quantification expands the understanding of the interdependencies within the modelled system.

## 1. INTRODUCTION

Direct use, single doublet geothermal systems are subject to several uncertainties. The impact of uncertainties can be significant for the lifetime of a geothermal system (Daniilidis et al., 2019, 2017, 2016). Consequently, the energy produced from the system is affected and that can have an impact on the economic performance (Daniilidis et al., 2017; C. J.L. Willems et al., 2017).

Moreover, the interference between adjacent doublets becomes more important, as direct use geothermal systems transition towards multiple doublets by a single operator (Daniilidis et al., 2019; Willems and Nick, 2019). Field development decisions are made at early stages, where uncertainties remain high and system behavior is not fully understood. Synthetic, representative models can aid in understanding the interplay between these uncertainties. Such models can be easily parametrizable and computationally efficient allowing the simulation of a multitude of realizations that would require unrealistically long computation time at full scale.

In this work synthetic representative models are used to explore the impact of a fault positioned between two doublets. The fault position and throw are altered. Additionally, the analysis considers two reservoir architecture configurations, two flow rates and two well configurations. All parameters combinations are tested in a comprehensive factorial experiment. The impact on system lifetime and produced cumulative energy is examined separately for each doublet, and also on the combination of both doublets.

## 2. METHODOLOGY

A Thermal Hydraulic (TH) model is developed using the Finite Element Method (FEM). The model conspires a reservoir with three layers of equal thickness.

**Table 1: Input considered in the analysis consisting of 128 reservoir simulations.**

Parameter	Values	Units
Fault Throw	50 ,75	(m)
Fault permeability	Normal to fault plane: $9.87 \times 10^{-18}$ (sealing – 0.01 mD), $4.93 \times 10^{-13}$ (conduit – 1 D) Fault plane: Normal to fault plane·10	(m <sup>2</sup> )
Reservoir layers (top to bottom)	min/mid/max, min/max/mid	-
Well configuration	Tram, Checkerboard	-
Flow rate	100, 250	m <sup>3</sup> /h
Well spacing	800	m
Top reservoir depth	2000	m
Fault distance	400, 200, 100, 50	m

The model considers a reservoir domain with a thickness of 150 m, comprised of three individual flow layers of 50 m thickness each, with homogenous flow properties (Figure 1). The top of the west part of the reservoir is situated at 2000 m depth. Over- and under-burden layers have a minimum thickness of 250 m. The whole domain (reservoir and over/under burden) is offset at the middle by a fault. The fault is a planar, vertical surface that extends 100 m above and below the reservoir layers. The throw of the fault takes different values. The inputs for the model are tabulated in **Error! Reference source not found.** and Table 2.

Two doublets are positioned in the system, one in the west and one in the east block of the model. The well spacing of the wells in a single doublet is 800 m and equals the spacing between the doublets, as this has been shown to be the most beneficial configuration for lifetime and NPV (Cees J.L. Willems et al., 2017). The well in a single doublet are oriented along the N-S direction. The west doublet has the producer on the north and injector on the south, while the east doublet has either the same (tram) or the opposite configuration (checkerboard) (see also Figure 3).

**Table 2: Reservoir layer flow properties**

Layer	Permeability (m <sup>2</sup> )	Porosity (%)
min	4.93×10 <sup>-13</sup> (5 mD)	17.2
mid	9.86×10 <sup>-14</sup> (100 mD)	18.5
max	4.93×10 <sup>-13</sup> (500 mD)	19.1
Over- & under- burden	9.86×10 <sup>-18</sup> (100 mD)	1

## 2.1 Reservoir model

A Thermal-Hydraulic model is built in COMSOL Multiphysics. The Energy Balance describes the heat transfer in the model as follows:

$$\rho C \frac{\partial T}{\partial t} + \rho_f C_f q \nabla T - \nabla(\lambda \nabla T) = 0 \quad (1)$$

in which T (K) is the temperature,  $\rho$  the mass density (kg/m<sup>3</sup>),  $C$  (J/(kg·K)) the specific heat capacity,  $\lambda$  (W/(m·K)) the thermal conductivity,  $q$  (m/s) the Darcy velocity and suffixes  $f$  and  $s$  refer to the fluid and the solid matrix respectively. The thermal conductivity and volumetric heat capacity of the system is computed based on the respective fluid and rock values separately according to:

$$\lambda = (1 - \phi)\lambda_s + \phi\lambda_f \quad (2)$$

and

$$\rho C = (1 - \phi)\rho_s C_s + \phi\rho_f C_f \quad (3)$$

in which  $\phi$  is rock porosity. The pressure field is computed based on the continuity equation according to:

$$\phi \frac{\partial \rho_f}{\partial t} + \nabla \cdot (\rho_f q) = 0 \quad (4)$$

where the flux  $q$  (m/s) is defined by Darcy's law:

$$q = -\frac{k}{\mu}(\nabla P - \rho_f g \nabla z) \quad (5)$$

in which  $k$  is the intrinsic porous medium permeability (m<sup>2</sup>),  $\mu$  the dynamic viscosity of the fluid (Pa·s),  $g$  the acceleration of gravity (m/s<sup>2</sup>) and  $P$  the hydraulic pressure (Pa).

The fluid density and viscosity are a function of temperature according to:

$$\rho_T = 838.466135 + 1.40050603 \cdot T - 0.0030112376 \cdot T^2 + 3.71822313 \cdot 10^{-7} \cdot T^3 \quad (6)$$

$$\mu_T = 1.3799566804 - 0.021224019151 \cdot T + 1.3604562827 \cdot 10^{-4} \cdot T^2 - 4.6454090319 \cdot 10^{-7} \cdot T^3 + 8.9042735735 \cdot 10^{-10} \cdot T^4 - 9.0790692686 \cdot 10^{-13} \cdot T^5 + 3.8457331488 \cdot 10^{-16} \cdot T^6 \quad (7)$$

The consideration for the mesh was to enable high enough result accuracy while maintaining a reasonable run time for the simulation ensemble. The model is meshed using a higher number of tetrahedral elements inside the reservoir layers, where flow is taking place (Figure 1). An additional refinement is performed around the wells where the higher Darcy velocities occur. Moreover, within the subdomain area (see Figure 1) a further refinement is applied ensuring a minimum of three vertical cells per reservoir layer. The minimum element size inside the reservoir domain is 5m and the maximum is 70m.

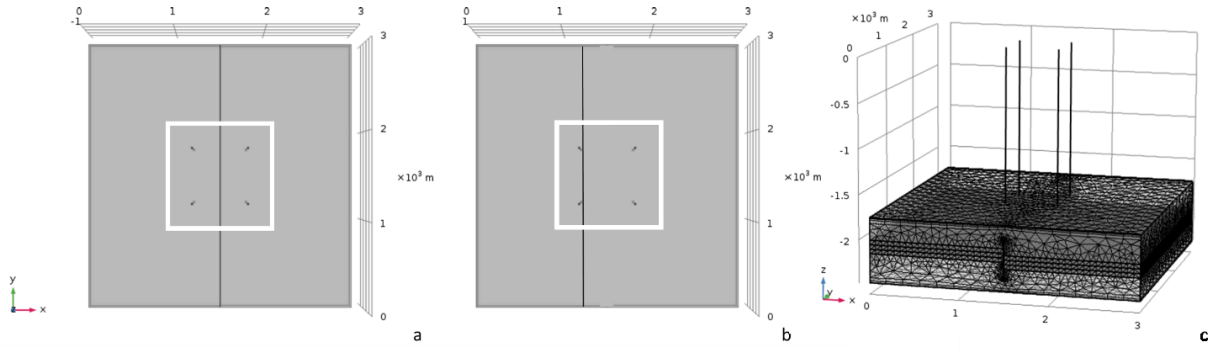


**Figure 1: Top view of the model with the fault positioned at the middle – 400 m (a) and 50 m away from the west doublet (b). The white highlighted area designates the influence area in which the HIP is calculated. The subdomain area size marked in white is two times the well spacing for both sides. Example of meshed domain for a horst type of faults in (c) angled view. The number of elements ranges between 180k to 310k depending on the geometry configuration.**

## 2.2 Well model

A simple well model is implemented in order to accommodate a flow rate control on the wells. The well rate is partitioned to each layer based on the ratio of the  $kh$  (permeability-thickness) of each layer to the  $kh$  of the whole reservoir interval as formulated in (Jalali et al., 2016) :

$$q_i = (k_i h_i / \sum_1^n k_i h_i) q_{total} \quad (8)$$

in which  $k_i$  ( $m^2$ ) and  $h_i$  (m) are the permeability and thickness of layer  $i$  respectively,  $n$  is the total number of layers and  $q_i$  and  $q_{total}$  are the layer  $i$  flow rate and the total flow rate respectively.

## 2.3 Initial and Boundary conditions

A geothermal gradient of 31 °C/km (Bonté et al., 2012) and a hydrostatic pressure gradient of 10 MPa/km are applied as initial conditions to the whole model domain. A pressure boundary condition is applied to the sides of the model, equal to the initial values calculated by through the hydrostatic pressure gradient.

The model boundary conditions for flow include no flow boundaries on the top and bottom surfaces of the model, while all side boundaries are open to flow. Temperature boundaries include a fixed temperature at the top and bottom of the model according to the initial conditions, while all side boundaries are open to heat transfer.

## 2.4 Heat In Place (HIP)

The calculation of the Heat In Place (HIP) is carried out according to :

$$HIP = \int_0^{V_{subdomain}} ((\rho_f c_f \phi + \rho_s c_s (1 - \phi))(T - T_{inj}) dV) \quad (9)$$

The HIP is calculated before any production takes place. The lower bound of the temperature difference is taken as  $T_{inj}$  as that is the lowest threshold that can effectively be recovered from the system (Garg and Combs, 2015). The HIP is calculated only inside the subdomain area (Figure 1).

## 2.5 System lifetime

In order to make the different models cross comparable the production temperature is normalized to the production temperature at  $t=0$  (see **Error! Reference source not found.**). The system lifetime is reached when thermal breakthrough occurs according to the condition for the temperature (°C) of the hot water from the production well

$$T_{prod_t} \leq 0.95 \cdot T_{prod_{t=0}} \quad (10)$$

is met. This condition is quite sensitive and is meant to capture the moment at which a slight change in the production temperature is measured. It therefore can be considered as worst case scenario for lifetime, bearing in mind that a temperature drop of less than 10 °C might still not compromise the operation of the geothermal system. The produced power used for the calculation of income is computed according to:

$$P_{well} = Q \rho_f c_f \Delta T \quad (11)$$

in which  $Q$  is the flow rate ( $m^3/s$ ) and  $\Delta T$  is the temperature difference between producer and injector wells (K). The required pump power only considers the pressure drop in the reservoir:

$$P_{pump} = \frac{\Delta P \cdot Q}{\eta} \quad (12)$$

where  $\Delta P$  is the pressure difference between the wells and  $\eta$  is the pump efficiency. The overall system power is then calculated as:

$$P_{system} = P_{well} - P_{pump}$$

(13)

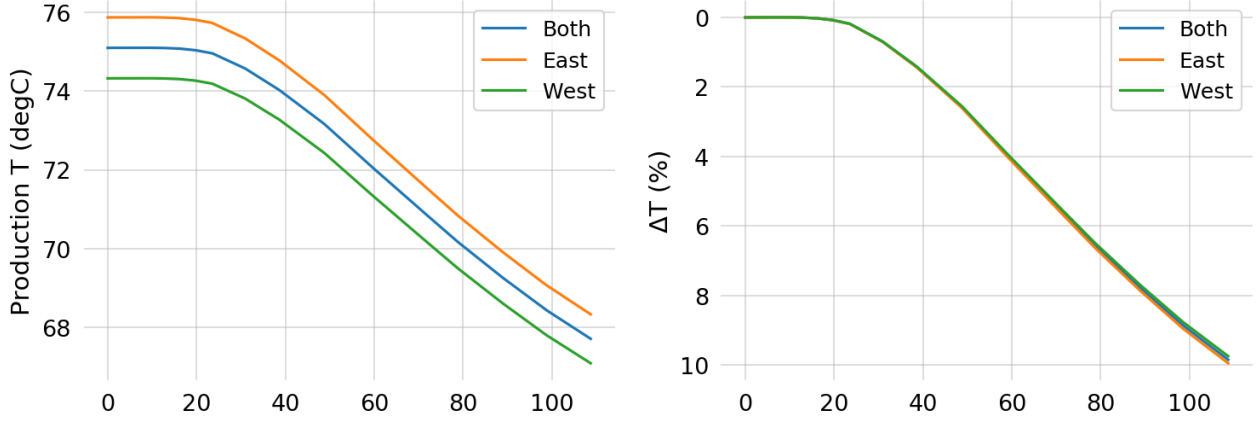


**Figure 2: Normalizing the production temperature to a percentage change compared to the initially produced temperature allows for cross comparison between different models.**

### 3. RESULTS

The impact of the different fault properties on the shape of the cold front is first showcased by examining the results of two individual simulations (Figure 3 and Figure 4). Both simulations exhibit identical inputs, with the fault permeability being the only difference. Following, the full dataset of 128 simulations is presented, drawing a comparison between each individual doublet and the aggregated performance of both doublets (Figure 5, Figure 6). Lastly, the sensitivity to the inputs used is shown (Figure 7, Figure 8 and Figure 9).

#### 3.1 Fault permeability impact

The flow properties of the fault have a major impact on the shape of the cold front. A sealing fault causes a clear distortion to the shape of the cold front (Figure 3). This distortion can be better observed in the respective cross sections of Figure 3. The absence of a flow path along the fault channels the flow of cold water from the injector along the fault plane. As a result, at the producer well the cold front arrives first from the side of the fault. Contrary to this, the outer side of the producer, away from the fault, maintains a higher temperature for a longer period of time. These results are consistent for both doublets, as the fault throw and respective depth of each block do not cause noticeable differences.

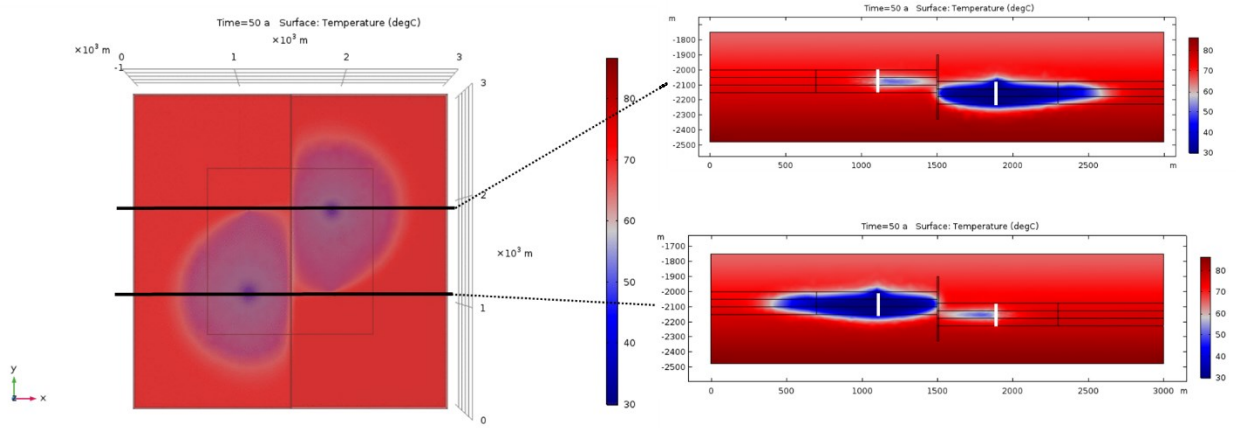
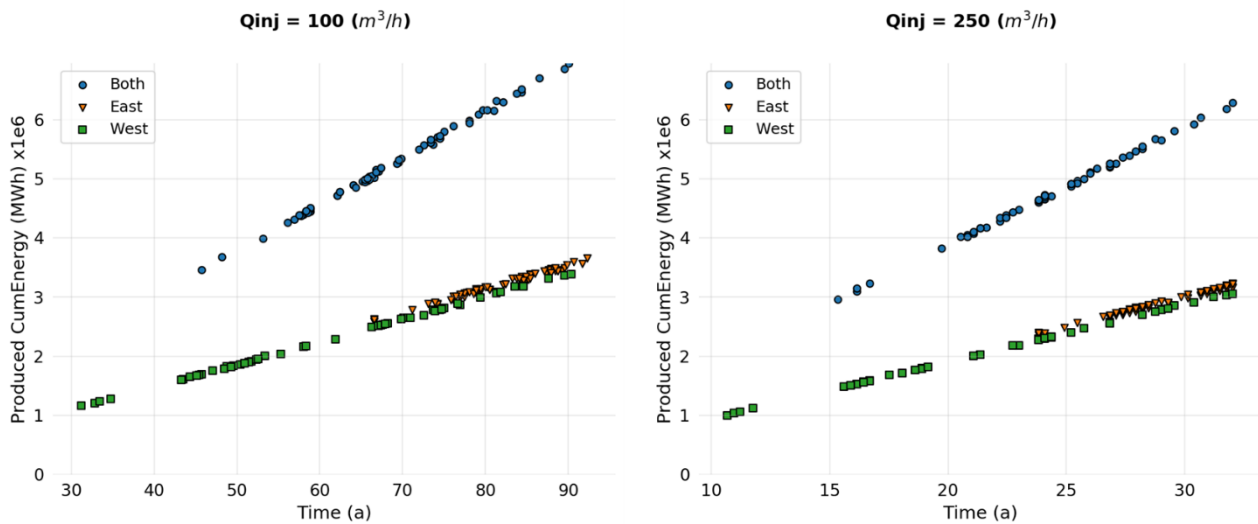


**Figure 3: Top view and respective sections through the west producer and east injector (North section) and the west injector and east producer (South section). The fault permeability is sealing , the throw of 75 m, the injection flow rate is 250 m<sup>3</sup>/h, the reservoir architecture is min/max/mid, while a checkerboard configuration is used for the well arrangement.**

A conduit flow provides a channelized path for the cold water to propagate into. This leads to flow along the fault that escapes out of the influence area of the doublets (Figure 4). At the same time the cold water flow also travels across the fault, preferentially using the highest flowing layer (in the case shown in Figure 4 the middle one). As a result, both injectors contribute cold water flow to both producers. The resulting cold water front shape after 50 years of production shows a characteristic tear shape point towards both producers.

### 3.2 Single developer – two individual developers

For two individual developers, the east doublet always exhibits a higher amount of cumulative energy produced; this is attributed to the fault offset that positions the east doublet deeper and therefore producing with slightly higher temperature, based on the geothermal gradient.



The percentage of recovered HIP compared to the initial HIP shows no difference between a single developer or two individual ones (Figure 6). This result is valid regardless of the flow rate used. Similarly, to the cumulative produced energy using a higher flow rate achieves comparable heat recovery at shorter lifetimes. However, low flow rates do result in higher minimum and maximum values of recovered HIP. This can be attributed to longer lifetimes enabling an increased contribution of heat recharge via conduction from the layers confining the reservoir.

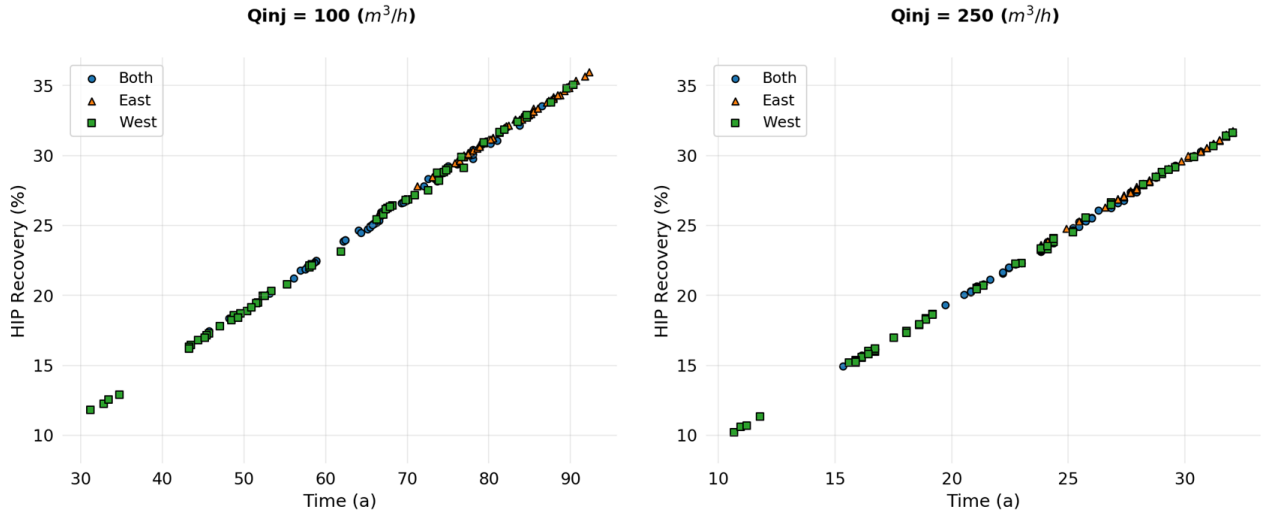


**Figure 6: Recovered HIP (%) at the time of breakthrough for the whole dataset of 128 simulations.**

### 3.3 Result sensitivity

The result sensitivity shown considers both doublets operated by a single developer. The system lifetime is most sensitive to the flow rate used, with high flow rates resulting in shorter system lifetime (Figure 7). Slightly improved lifetime is achieved for the checkerboard configuration although in some cases a tramline configuration may lead to slightly longer lifetime. A conduit fault showcases a wider distribution of system lifetimes than a sealing one and can potentially lead to both shorter and longer lifetimes compared to the latter. The fault throw however shows minor changes in lifetimes. Reservoir architecture favors having the most permeable layer at the bottom of the reservoir, yielding a slightly shifted upwards distribution, compared to having the most permeable layer at the middle of the reservoir. Lastly, fault distance exhibits a very similar distribution for all values that is gradually shifted upwards when the fault is progressively further away from the west doublet.

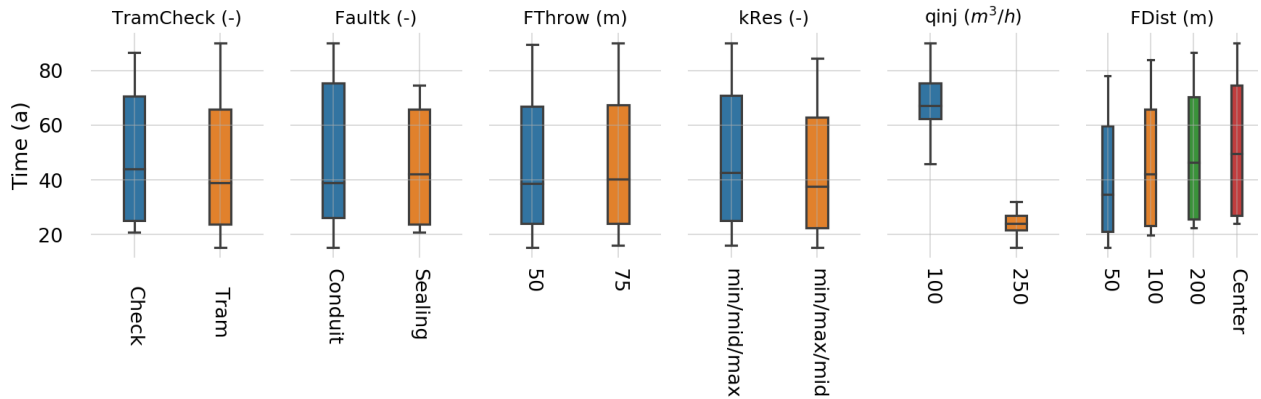


**Figure 7: Sensitivity of the thermal breakthrough time to the input parameters**

The generated cumulative energy and HIP recovery show almost identical sensitivities to the input parameters (Figure 8 and Figure 9). The checkerboard well configuration demonstrates a narrower distribution with higher values for both cumulative energy and HIP recovery compared to the tram configuration. A sealing fault behavior showcases also a narrower distribution meaning that its impact is quite dominant on the outcome; at the same time the wider distribution of a conduit fault allows for both lower and higher amounts of generated energy and heat recovery with the median being significantly higher compared to a sealing fault. Contrary, the fault throw has a minor effect, with a higher throw resulting in a slight increase of the median values for both produced and recovered energy. Similar to the system lifetime a reservoir architecture with the highest flowing layer at the bottom benefits energy production and recovery, but compared to lifetime this positive difference is more pronounced. Both flow rates show similar distribution values with higher flowrates resulting to notable lower energy production and recovery. Finally, the fault distance affects energy production and recovery in a similar way to its effect on system lifetime exhibiting higher values when moving further away from west doublet. However, in this case the distributions are narrower and the differences between each fault position more substantial.

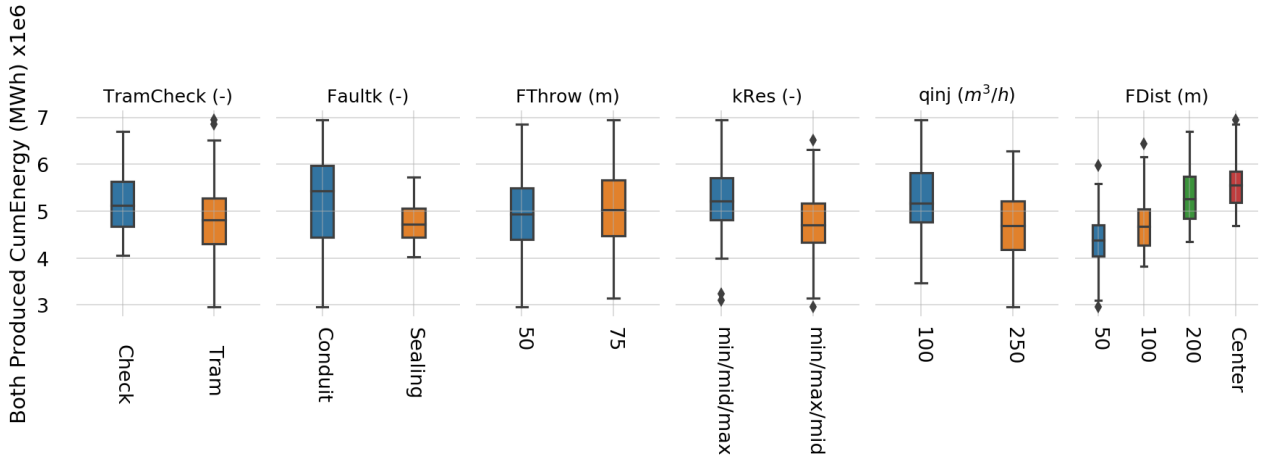


**Figure 8: Sensitivity of the produced cumulative energy (MWh) to the input parameters**

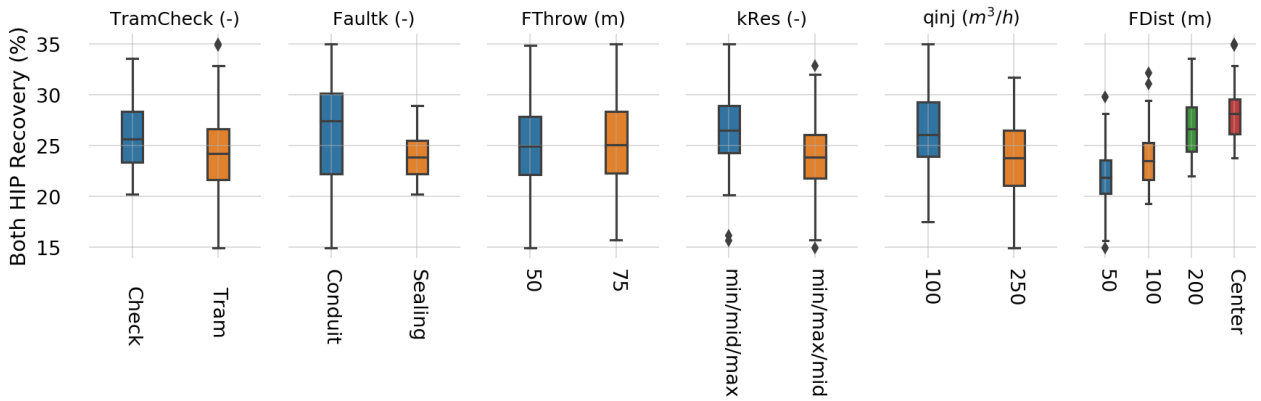


**Figure 9: Sensitivity of the HIP recovery (%) to the input parameters**

#### 4. DISCUSSION

Overall, the proposed analysis framework allows for identifying the importance and classifying the relative impact of the known unknowns for geothermal direct use systems. The results of this study demonstrate a discrepancy between the impact of various uncertainties to different evaluation indexes. Heat generation and recovery show quite different sensitivities to the considered uncertainties compared to system lifetime. Extending system lifetime is often considered synonymous to improving the energy production from a given system, these results suggest this is not a linear relationship.

Specifically, the impact of the fault proximity to the west doublet and the flow behavior of the fault emerge as crucial aspects of this analysis, while the fault throw is less significant. This highlights the point that identifying the presence of faults and evaluating their flow behavior is of high importance for a robust estimation of both system lifetime and generated energy.

Heat recovery within a certain influence area is pertinent as exploitation licenses are often restricted within boundaries. It is therefore of importance to consider these effects for both single developers with limited license extents but also larger developers with multiple systems and larger concessions. For the former the confines might dictate their development plans altogether while that latter might further refine their development plans at the edges of their concessions where interferences with neighboring licenses become pertinent.

The benefits of simple models that can be easily parametrized is demonstrated. With little effort the scope of this type of analysis can be either extended or further sharpened to aid more robust decision making. The flexibility arises from the small model size and linear scaling with the number of available computational resources. This in turn allows to sharply test concepts that can be applied at the field scale with models that are faster to run and yield a comprehensive parametric study overview of the identified possibilities of parameter values. Specifically for larger models containing multiple doublets this approach can be very beneficial compared to running a full uncertainty quantification workflow at the field scale.

The impact of the above to the NPV have not been discussed as that falls beyond the scope of the current study. It would however be interesting to further evaluate how the balance between system lifetime and generated energy reflects on the economic output of single developers with multiple doublets against multiple developers with one doublet each.

## 5. CONCLUSIONS

In the paper an ensemble of synthetic models is used to examine the combined impact of well configuration, fault flow properties and throw, reservoir architecture, flow rate and distance to fault of a two doublet system for direct use geothermal energy. The synthetic models used are easily parametrizable, while the analysis benefits linearly with the amount of available computational resources. The analysis considers the impact of the aforementioned parameters to the system lifetime, energy generation and HIP recovery, comparing two development scenarios: a single developer operating both doublets against two individual developers with a single doublet each.

The analysis identifies flowrate, fault flow behavior and fault proximity to the west doublet as then main factors affecting both system lifetime, as well as energy production and recovery. The fault permeability combined with the doublet positioning with regards to the fault suggests that it is crucial to characterize the presence and flow properties of the fault for generating robust development plans. The impact of the fault throw however is found to be negligible.

Importantly, for system lifetime the effect of the flow rate is dominant with other parameters exhibiting a smaller influence. Energy production and recovery exhibit a very similar sensitivity pattern between them but quite different than the one for system lifetime. Particularly, while the same parameters are more dominant, the impact of flow rate is not as pronounced and fault permeability, well configuration, reservoir architecture emerge as important factors. Future efforts should be directed to illuminate how the different sensitivities in system lifetime and energy production coalesce to the generated NPV.

## REFERENCES

- Bonté, D., Wees, J.D. Van, Verweij, J.M., 2012. Subsurface temperature of the onshore Netherlands: new temperature dataset and modelling. *Netherlands J. Geosci. en Mijnb.* 91, 491–515.
- Daniilidis, A., Alpsy, B., Herber, R., 2017. Impact of technical and economic uncertainties on the economic performance of a deep geothermal heat system. *Renew. Energy* 114, 805–816. <https://doi.org/10.1016/j.renene.2017.07.090>
- Daniilidis, A., Doddema, L., Herber, R., 2016. Risk assessment of the Groningen geothermal potential: From seismic to reservoir uncertainty using a discrete parameter analysis. *Geothermics* 64, 271–288. <https://doi.org/http://dx.doi.org/10.1016/j.geothermics.2016.06.014>
- Daniilidis, A., Nick, H.M., Bruhn, D., 2019. Parameter Interdependency In Energy And Economic Output Of A Geothermal Development Strategy, in: *European Geothermal Congress. EGC, The Hague*, pp. 1–5.
- Garg, S.K., Combs, J., 2015. A reformulation of USGS volumetric “heat in place” resource estimation method. *Geothermics* 55, 150–158. <https://doi.org/10.1016/J.GEOTHERMICS.2015.02.004>
- Jalali, M., Embry, J.-M., Sanfilippo, F., Santarelli, F.J., Dusseault, M.B., 2016. Cross-flow analysis of injection wells in a multilayered reservoir. *Petroleum* 2, 273–281. <https://doi.org/10.1016/J.PETLM.2016.05.005>
- Willems, C.J.L., Nick, H.M., 2019. Towards optimisation of geothermal heat recovery: An example from the West Netherlands Basin. *Appl. Energy* 247, 582–593. <https://doi.org/10.1016/J.APENERGY.2019.04.083>
- Willems, C. J.L., Nick, H.M., Goense, T., Bruhn, D.F., 2017. The impact of reduction of doublet well spacing on the Net Present Value and the life time of fluvial Hot Sedimentary Aquifer doublets. *Geothermics* 68, 54–66. <https://doi.org/10.1016/j.geothermics.2017.02.008>
- Willems, Cees J.L., Nick, H.M., Weltje, G.J., Bruhn, D.F., 2017. An evaluation of interferences in heat production from low enthalpy geothermal doublets systems. *Energy* 135, 500–512. <https://doi.org/10.1016/j.energy.2017.06.129>